



**HAL**  
open science

## Effect of residual stress on energy storage property in PbZrO<sub>3</sub> antiferroelectric thin films with different orientations

J. Ge, Denis Remiens, J. Costecalde, Y. Chen, X.L. Dong, G.S. Wang

► **To cite this version:**

J. Ge, Denis Remiens, J. Costecalde, Y. Chen, X.L. Dong, et al.. Effect of residual stress on energy storage property in PbZrO<sub>3</sub> antiferroelectric thin films with different orientations. Applied Physics Letters, 2013, 103 (16), pp.162903. 10.1063/1.4825336 . hal-00877658

**HAL Id: hal-00877658**

**<https://hal.science/hal-00877658>**

Submitted on 27 May 2022

**HAL** is a multi-disciplinary open access archive for the deposit and dissemination of scientific research documents, whether they are published or not. The documents may come from teaching and research institutions in France or abroad, or from public or private research centers.

L'archive ouverte pluridisciplinaire **HAL**, est destinée au dépôt et à la diffusion de documents scientifiques de niveau recherche, publiés ou non, émanant des établissements d'enseignement et de recherche français ou étrangers, des laboratoires publics ou privés.

# Effect of residual stress on energy storage property in $\text{PbZrO}_3$ antiferroelectric thin films with different orientations

Cite as: Appl. Phys. Lett. **103**, 162903 (2013); <https://doi.org/10.1063/1.4825336>

Submitted: 14 July 2013 • Accepted: 01 October 2013 • Published Online: 16 October 2013

Jun Ge, Denis Remiens, Jean Costecalde, et al.



View Online



Export Citation



CrossMark

## ARTICLES YOU MAY BE INTERESTED IN

[Enhancement of energy storage in epitaxial  \$\text{PbZrO}\_3\$  antiferroelectric films using strain engineering](#)

Applied Physics Letters **105**, 112908 (2014); <https://doi.org/10.1063/1.4896156>

[Composition-dependent dielectric and energy-storage properties of  \$\(\text{Pb},\text{La}\)\(\text{Zr},\text{Sn},\text{Ti}\)\text{O}\_3\$  antiferroelectric thick films](#)

Applied Physics Letters **102**, 163903 (2013); <https://doi.org/10.1063/1.4802794>

[Flexible high energy density capacitors using La-doped  \$\text{PbZrO}\_3\$  anti-ferroelectric thin films](#)

Applied Physics Letters **112**, 092901 (2018); <https://doi.org/10.1063/1.5018003>

Lock-in Amplifiers  
up to 600 MHz



Zurich  
Instruments



## Effect of residual stress on energy storage property in PbZrO<sub>3</sub> antiferroelectric thin films with different orientations

Jun Ge,<sup>1</sup> Denis Remiens,<sup>2</sup> Jean Costecalde,<sup>2</sup> Ying Chen,<sup>1</sup> Xianlin Dong,<sup>1</sup> and Genshui Wang<sup>1,a)</sup>

<sup>1</sup>Key Laboratory of Inorganic Functional Materials and Devices, Shanghai Institute of Ceramics, Chinese Academy of Sciences, 1295 Dingxi Road, Shanghai 200050, People's Republic of China

<sup>2</sup>IEMN-DOAE-MIMM, CNRS UMR 8520, Université de Valenciennes et du Hainaut Cambrésis, 59313 Valenciennes Cedex 9, Cité scientifique, 59655 Villeneuve-d'Ascq Cedex, France

(Received 14 July 2013; accepted 1 October 2013; published online 16 October 2013)

The effect of residual stress on energy storage property was investigated for a series of PbZrO<sub>3</sub> thin films on SrTiO<sub>3</sub> and Si substrates. Compressive or tensile residual stress influences the critical electric field  $E_A$  for the ferroelectric-to-antiferroelectric phase transition, thus for films with (110)/(101) orientation, energy density  $W$  of films on SrTiO<sub>3</sub> is 38% larger than films on Si; in contrast, (001)-oriented PbZrO<sub>3</sub> films on SrTiO<sub>3</sub> show slightly smaller  $W$  compared to films on Si. We conclude that the different responses of  $W$  to stress are related to the different constrain states in films with different orientations. © 2013 AIP Publishing LLC. [<http://dx.doi.org/10.1063/1.4825336>]

Dielectric materials that provide the capability of high-performance energy storage are of great importance for the power electronics in a wide range of technological applications. Among various dielectric materials, antiferroelectrics (AFE) are promising candidates for dielectrics in high energy density electrical capacitors due to the field-induced phase transition into the ferroelectric state accompanied by large charge storage. In general, the recoverable energy density ( $W$ ) can be calculated by the integral  $W = \int E dD$ , where  $E$  is the electric field and  $D$  is the electric displacement or charge density. Therefore, antiferroelectric thin films can develop greatly enhanced energy density compared with their bulk counterparts because they typically have higher dielectric strength and the electric displacement tends to saturate at higher electric field.<sup>1,2</sup> To further enhance the energy storage property of AFE film, much effort has been made including modification of film composition,<sup>3-8</sup> PbO content excess,<sup>9,10</sup> and using oxide top electrodes.<sup>11</sup> It was reported that a very high energy density of 37 and 56 J/cm<sup>3</sup> can be obtained in Pb<sub>0.92</sub>La<sub>0.08</sub>(Zr<sub>0.95</sub>Ti<sub>0.05</sub>)O<sub>3</sub> and Pb<sub>0.97</sub>La<sub>0.02</sub>(Zr<sub>0.55</sub>Sn<sub>0.40</sub>Ti<sub>0.05</sub>)O<sub>3</sub> AFE films, respectively.<sup>4,8</sup>

Very recently, it has been shown experimentally that  $E_F$  for the antiferroelectric-to-ferroelectric phase transition and  $E_A$  for the reverse transition have been shifted to higher levels by compressive stresses in the Nb-doped lead zirconate titanate stannate (PNZST) bulk ceramic,<sup>12,13</sup> thus lead to an increase in the energy density of antiferroelectric capacitor. As a result, one may wonder if the stress, which is generally existed in films and can be controlled by a lot of parameters such as the choice of substrate, bottom electrode, annealing temperature, texture orientation, and so on can also influence the energy storage property of AFE films. However, reports on the effect of stress on polarization switching and energy storage properties in AFE films are rather limited so far. Xu *et al.* studied the field-induced phase switching of (111)-oriented lead zirconate titanate stannate (PZST) thick films on Si substrate and concluded that the tensile stress due to the thermal mismatch between film and substrate would

make the films prone to the FE phase.<sup>14,15</sup> However, it appears that no report on strain dependency of AFE films on different substrates has been published. Hence, in this study, PbZrO<sub>3</sub> thin films, which are the prototype of AFE films, were deposited on LaNiO<sub>3</sub> (LNO) buffered SrTiO<sub>3</sub> and SiO<sub>2</sub>/Si substrates and their strain-induced structure property and energy storage property as a function of temperature have been investigated.

The PZ/LNO heterostructures were grown on (001) SrTiO<sub>3</sub> and SiO<sub>2</sub>/Si substrates by off-axis rf magnetron sputtering. The LNO electrodes were deposited at different oxygen partial pressure ( $O_2/Ar + O_2 = 0\%$  and  $20\%$ , respectively) so that for the same LNO different orientations and lattice constants can be achieved.<sup>16</sup> 340-nm-thick PZ films were then deposited on LNO buffered SiO<sub>2</sub>/Si and SrTiO<sub>3</sub> substrates using a 3-in.-diamater PbZrO<sub>3</sub> target made by uniaxial pressed mixed PbO and ZrO<sub>2</sub> powders in stoichiometric composition. The films were deposited on unheated substrate holder under the total pressure of  $1 \times 10^{-2}$  mbar ( $\sim 1$  Pa) (100% argon), with RF-power of 1.32 W/cm<sup>2</sup>, and the target-substrate distance is 60 mm. These growth conditions yielded a deposition rate of about 570 Å/h for the PZ layer. The as-deposited films were amorphous and a post annealing treatment under air atmosphere at 625 °C was performed to crystallize the films into the perovskite phase.

The structure and phase purity of the films were checked using Rigaku SmartLab high resolution X-ray diffractometer (HRXRD). LNO top electrode (diameter of  $\sim 140 \mu\text{m}$ ) was deposited by rf magnetron sputtering at RT through a photolithography process. The thickness of LNO top electrode is about 100 nm. The hysteresis loops were performed by aixACCT TF2000FE equipment.

Figure 1 shows X-ray diffraction (XRD, CuK <sub>$\alpha$</sub>  radiation) patterns of PZ films deposited on LNO-buffered (001) SrTiO<sub>3</sub> and SiO<sub>2</sub>/Si substrates. It should be noted that PZ possesses an orthorhombic structure below curie temperature ( $\sim 230$  °C) in which the orthorhombic cell is a multiple unit cell and contains eight primitive cells, which have a tetragonal structure ( $a_0 = \sim 4.15$  Å,  $b_0 = \sim 4.15$  Å, and  $c_0 = \sim 4.10$  Å). Hence, for

<sup>a)</sup>Electronic mail: genshuiwang@mail.sic.ac.cn

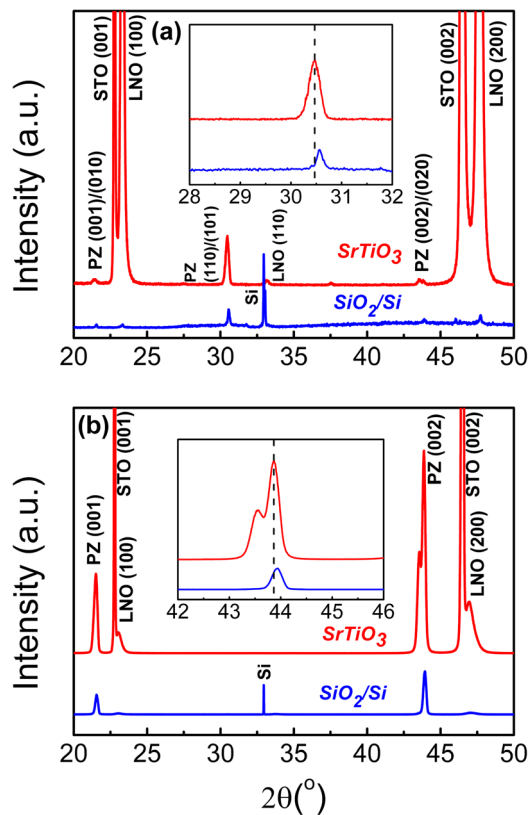


FIG. 1. Room temperature XRD  $\theta$ - $2\theta$  of PZ films grown on (a) LNO (0% oxygen partial pressure) buffered (001) SrTiO<sub>3</sub> and SiO<sub>2</sub>/Si, (b) LNO (20% oxygen partial pressure) buffered (001) SrTiO<sub>3</sub> and SiO<sub>2</sub>/Si.

convenience all the peaks of PZ films are indexed based on the tetragonal structure. In Fig. 1(a), it is shown that LNO deposited on SrTiO<sub>3</sub> at 0% oxygen partial pressure is highly (100)-oriented, while on SiO<sub>2</sub>/Si shows a (110)-preferred orientation. However, PZ films on both substrates have (110)/(101) preferred orientation and the reflections from the LNO electrodes indicate an out-of-plane lattice constant of 3.81 Å. The fact that PZ does not follow the (100) orientation of LNO on SrTiO<sub>3</sub> is maybe due to the large lattice misfit between LNO (3.81 Å) and PZ (~4.14 Å as a pseudo-cubic), which makes it difficult to facilitate grain-on-grain growth. In contrast, Fig. 1(b) shows LNO films deposited at 20% oxygen partial pressure are all highly (100)-oriented and yield a lattice constant of 3.87 Å, which indicates smaller lattice misfit with the overlaying PZ film. Consequently, PZ films follow the (100) orientation of LNO and show highly (001)-oriented fiber texture on both substrates. The out-of-plane  $c$  parameter of films with (001) orientation is 4.107 Å on SiO<sub>2</sub>/Si substrates (calculated from the (002) peak from XRD patterns) and as on SrTiO<sub>3</sub> substrates, the (002) peak is more split, with a lattice parameter about 4.113 Å from the dominant peak, indicating the  $c_0$  axis of the PZ unit cell lies perpendicular to the film plane and the  $a_0$  and  $b_0$  axes lie in plane. In addition, the rocking curve and  $\Phi$ -scan confirm that PZ with LNO electrode deposited at 20% O<sub>2</sub> partial pressure on SrTiO<sub>3</sub> are epitaxially grown and the other PZ films are uniaxially textured.<sup>16</sup> Moreover, as we can see from the insets of Fig. 1, the peaks corresponding to PZ shift towards lower  $2\theta$  angle as the substrates change from Si to SrTiO<sub>3</sub>, indicating an increase in the out-of-plane lattice parameter, which means films on SrTiO<sub>3</sub>

receive a higher compressive stress compared to films on Si substrate.

In general, stress in a thin film can come from various sources including (1) intrinsic stress induced from a particular growth process, (2) transformation stress due to structural phase transition, (3) lattice mismatch stress due to epitaxial growth, and (4) thermal stress due to thermal expansion mismatch. Because all PZ films are deposited using the same parameters and the phase structures are essentially similar, the intrinsic and transformation stress can be treated as the same for all samples. Considering the thermal stress, the thermal expansion coefficients (TECs) of SrTiO<sub>3</sub> and SiO<sub>2</sub>/Si substrates are 11.0<sup>17</sup> and 2.6<sup>14</sup> ppm/K, respectively, and assuming PZ films have a same value of TEC as PZ bulk ceramic (8.0<sup>18</sup> ppm/K), thus films on SrTiO<sub>3</sub> and SiO<sub>2</sub>/Si are under compressive and tensile stress, respectively. As for lattice misfit stress, in view of only PZ films on LNO (20% of oxygen partial pressure) buffered SrTiO<sub>3</sub> were epitaxially grown and lattice parameter of LNO (3.87 Å) is smaller than that of PZ, it seems that the film will receive additional epitaxial compressive stress. However, there are also some reports argue that in epitaxial Pb(Zr<sub>1-x</sub>Ti<sub>x</sub>)O<sub>3</sub> (PZT) films much thicker than the critical thickness (>80 nm), the lattice strain is completely relaxed.<sup>17,19</sup>

Polarization versus electric field hysteresis loops were measured on all four samples at a series of temperatures. Figures 2(a) and 2(b) show the loops of PZ films at 30 and 110 °C with a peak field of 700 kV/cm. It can be seen that with the temperature increasing, both critical electric fields  $E_F$  and  $E_A$  shift to lower value leading to a decrease in  $W$ , which is similar to our previous report on

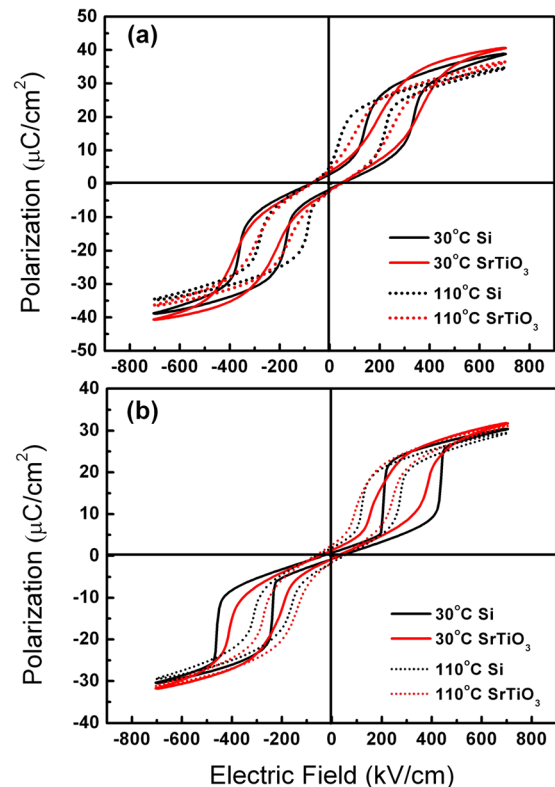


FIG. 2. Polarization versus electric field hysteresis loops of (a) (110)/(101)-oriented PZ films and (b) (001)-oriented PZ films on SiO<sub>2</sub>/Si and SrTiO<sub>3</sub> at 30 and 110 °C (measured at 100 Hz).



$\text{Pb}_{0.97}\text{La}_{0.02}(\text{Zr}_{0.95}\text{Ti}_{0.05})\text{O}_3$  AFE films.<sup>11</sup> The effect of residual stress can be verified by the comparison of hysteresis loops of films on different substrates at the same temperature. It can be concluded that with the same orientation, films on  $\text{SrTiO}_3$  appear to have slightly higher maximum polarization compared to films on  $\text{SiO}_2/\text{Si}$ . This is believed to result from the polarization rotating towards the film plane with tensile stress.<sup>17</sup> However, the relationships of  $E_F$  and  $E_A$  with thermal stress vary substantially as the orientations of films change. For PZ samples with (110)/(101) preferred orientation, the  $E_F$  and  $E_A$  of the sample on  $\text{SrTiO}_3$  are slightly higher than that of the sample on  $\text{SiO}_2/\text{Si}$ . Considering the films on  $\text{SrTiO}_3$  receive higher compressive stress, it is consistent with the report we mentioned before on PNZST AFE bulk ceramic<sup>13</sup> under compressive stresses. In contrast, when the orientation of PZ films changes to (001), our observation shows an opposite trend that the films on  $\text{SrTiO}_3$  display lower  $E_F$  and  $E_A$  compared to films on  $\text{SiO}_2/\text{Si}$ . Furthermore, the phase transitions (both forward and reverse ones) appear to be more abrupt in sample on  $\text{SiO}_2/\text{Si}$  substrate.

From the hysteresis loops data at different electric fields and temperatures, energy storage density can be further extracted (Fig. 3). For samples with (110)/(101) orientation, films on  $\text{SrTiO}_3$  substrate exhibit higher energy density in whole temperature range compared to films on  $\text{SiO}_2/\text{Si}$ , which means the compressive stresses enhance energy density of PZ films. For example, at  $30^\circ\text{C}$ ,  $W$  at  $700\text{ kV/cm}$  is  $\sim 9.0\text{ J/cm}^3$  in films on  $\text{SrTiO}_3$  and  $\sim 6.5\text{ J/cm}^3$  in films on  $\text{SiO}_2/\text{Si}$ , corresponding to a 38% increase. In contrast, for samples with (001) orientation, slightly higher energy

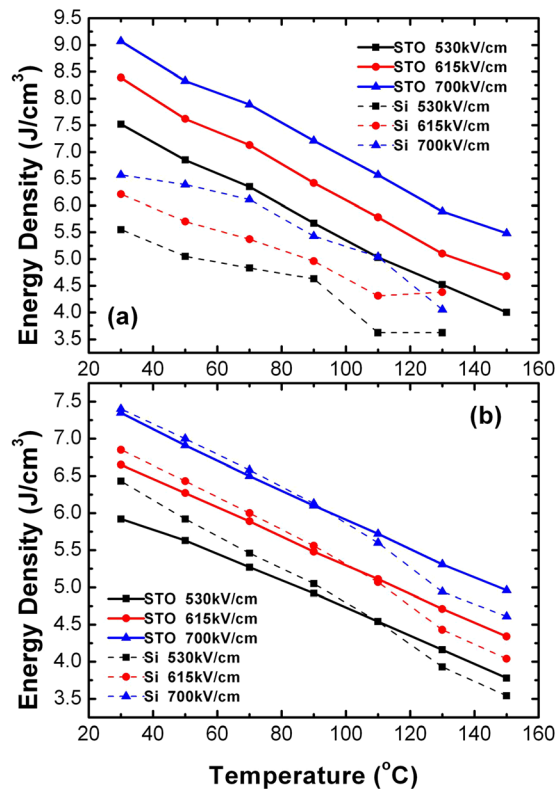


FIG. 3. The temperature dependence of  $W$  for (a) (110)/(101)-oriented PZ films and (b) (001)-oriented PZ films on  $\text{SiO}_2/\text{Si}$  and  $\text{SrTiO}_3$  measured at 530, 615, and  $700\text{ kV/cm}$ , respectively.

density is achieved in films on  $\text{SiO}_2/\text{Si}$  compared to films on  $\text{SrTiO}_3$  at room temperature, especially at relatively low electric field. For instance at  $30^\circ\text{C}$ ,  $W$  is  $\sim 6\text{ J/cm}^3$  in films on  $\text{SrTiO}_3$  and  $\sim 6.5\text{ J/cm}^3$  in films on  $\text{SiO}_2/\text{Si}$  at  $530\text{ kV/cm}$ . However, as the temperature increases, the energy density of films on  $\text{SiO}_2/\text{Si}$  decreases a little more rapidly and hence becomes smaller than that of films on  $\text{SrTiO}_3$  at temperatures above  $110^\circ\text{C}$ .

The fact that the PZ films with (110)/(101) orientation give larger energy density on  $\text{SrTiO}_3$ , while films with (001) orientation obtain better energy storage property on  $\text{SiO}_2/\text{Si}$ , can be explained by a consideration of the different constraint states in films with different orientations. Based on the model of Xu *et al.*,<sup>14</sup> we draw the schematic diagram of the primitive cells in AFE and FE phases with different orientations (Figure 4). The polar direction of the antiparallel dipoles is along the  $[110]$  direction of the tetragonal primitive cell. When changed to the FE phase, the tetragonal primitive cell becomes rhombohedral with the polar directions along the  $[111]$  direction. The lattice angle of the unit cell of the FE rhombohedral phase  $\alpha_{\text{Rh}}$  is very close to  $90^\circ$  ( $89.8^\circ$  or  $89.95^\circ$ ). The lattice parameter  $a_{\text{Rh}}$  of FE rhombohedral phase is a little smaller than  $a_{\text{tet}}$  of the AFE tetragonal primitive cell, but obviously larger than  $c_{\text{tet}}$ . Fig. 4(a) shows the

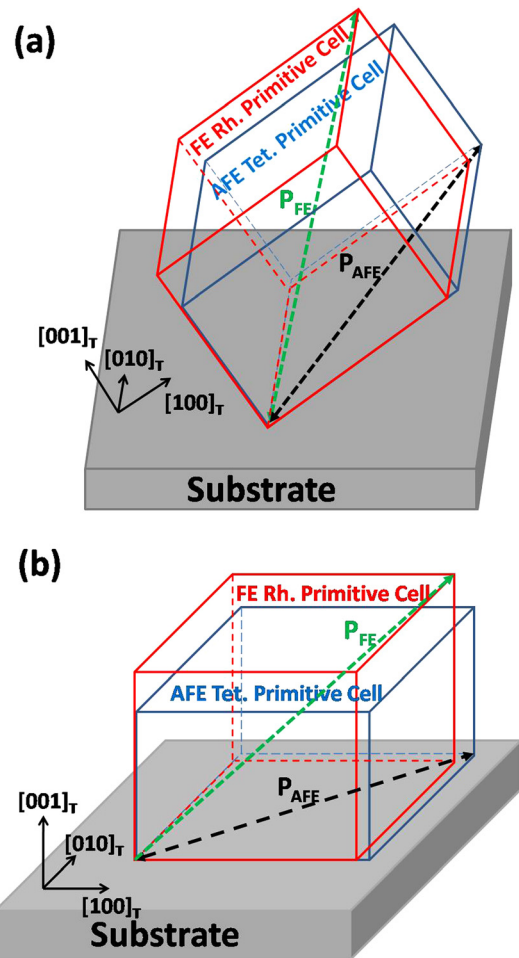


FIG. 4. Schematic diagram of the primitive cells with (a) (110) orientation and (b) (001) orientation in AFE and FE phases. The primitive cell is tetragonal (Tet.) structure in AFE phase and rhombohedral (Rh.) structure in FE phase.

primitive cells with (101) orientation in AFE and FE phases. The situation of primitive cells with (110) orientation would be similar. It can be seen that the films will expand in the plane parallel to the film surface after being switched to the FE phase. Hence, the residual compressive stress will make the films prone to the AFE phase, thus shifts the  $E_F$  and  $E_A$  to higher value. In contrast, if the films are (001)-oriented, as shown in Fig. 4(b), because  $a_{Rh}$  is a little smaller than  $a_{tet}$ , the films will contract along the in-plane direction and hence it is not compressive stress but tensile stress that will stabilize the AFE phase, leading to an increase in  $E_F$  and  $E_A$  of samples on  $SiO_2/Si$  in comparison to samples on  $SrTiO_3$ .

In summary, we have grown (110)/(101)- and (001)-oriented PZ films on both LNO buffered  $SrTiO_3$  and  $SiO_2/Si$  substrates. It is observed that the critical electric fields  $E_F$  and  $E_A$  of films with (110)/(101) orientation increase as the substrate changes from  $SiO_2/Si$  to  $SrTiO_3$  substrates, which lead to a higher energy density in films on  $SrTiO_3$  substrate. However, for films with (001) orientation, the  $E_F$  and  $E_A$  decrease in films on  $SrTiO_3$  substrate, which results in a higher energy density in films on  $SiO_2/Si$  substrate. These results demonstrate that the orientation of PZ films may heavily influence the relation between the energy density property and the stress field within the PZ films. We conclude that it is closely related to the different constrain states in films with different orientations.

The authors would like to thank Dr. Yves Sama and Dr. Pascal Roussel for their support for sputtering process and HRXRD measurements, respectively. This work was supported by NSAF (No. U1330128), National important basic research project (2012CB619406), Open Project Key Laboratory of Polar Materials and Devices Ministry of

Education (Grant No. KFKT20120001), and International Partnership Project of Chinese Academy of Science.

- <sup>1</sup>K. Yao, S. Chen, M. Rahimabady, M. S. Mirshekarloo, S. Yu, F. E. Tay, T. Sritharan, and L. Lu, *IEEE Trans. Ultrason. Ferroelectr. Freq. Control* **58**(9), 1968 (2011).
- <sup>2</sup>M. McMillen, A. M. Douglas, T. M. Correia, P. M. Weaver, M. G. Cain, and J. M. Gregg, *Appl. Phys. Lett.* **101**(24), 242909 (2012).
- <sup>3</sup>J. Parui and S. B. Krupanidhi, *Appl. Phys. Lett.* **92**(19), 192901 (2008).
- <sup>4</sup>B. Ma, D.-K. Kwon, M. Narayanan, and U. Balachandran, *J. Mater. Res.* **24**(9), 2993 (2009).
- <sup>5</sup>X. Hao, J. Zhai, and X. Yao, *J. Am. Ceram. Soc.* **92**(5), 1133 (2009).
- <sup>6</sup>M. Sharifzadeh Mirshekarloo, K. Yao, and T. Sritharan, *Appl. Phys. Lett.* **97**(14), 142902 (2010).
- <sup>7</sup>M. Ye, Q. Sun, X. Chen, Z. Jiang, and F. Wang, *J. Am. Ceram. Soc.* **94**(10), 3234 (2011).
- <sup>8</sup>X. Hao, Y. Wang, L. Zhang, L. Zhang, and S. An, *Appl. Phys. Lett.* **102**(16), 163903 (2013).
- <sup>9</sup>X. Hao, J. Zhou, and S. An, *J. Am. Ceram. Soc.* **94**(6), 1647 (2011).
- <sup>10</sup>Y. Wang, X. Hao, and J. Xu, *J. Mater. Res.* **27**(13), 1770 (2012).
- <sup>11</sup>J. Ge, X. Dong, Y. Chen, F. Cao, and G. Wang, *Appl. Phys. Lett.* **102**(14), 142905 (2013).
- <sup>12</sup>X. Tan, J. Frederick, C. Ma, E. Aulbach, M. Marsilius, W. Hong, T. Granzow, W. Jo, and J. Rödel, *Phys. Rev. B* **81**(1), 014103 (2010).
- <sup>13</sup>S. E. Young, J. Y. Zhang, W. Hong, and X. Tan, *J. Appl. Phys.* **113**(5), 054101 (2013).
- <sup>14</sup>B. M. Xu, Y. H. Ye, and L. E. Cross, *J. Appl. Phys.* **87**(5), 2507 (2000).
- <sup>15</sup>B. M. Xu, X. H. Ye, Q. M. Wang, N. G. Pai, and L. E. Cross, *J. Mater. Sci.* **35**(23), 6027 (2000).
- <sup>16</sup>L. Yang, G. Wang, C. Mao, Y. Zhang, R. Liang, C. Soyer, D. Rémiens, and X. Dong, *J. Cryst. Growth* **311**(17), 4241 (2009); also See supplementary material at <http://dx.doi.org/10.1063/1.4825336> for detailed information of structure property.
- <sup>17</sup>M. D. Nguyen, M. Dekkers, E. Houwman, R. Steenwelle, X. Wan, A. Roelofs, T. Schmitz-Kempen, and G. Rijnders, *Appl. Phys. Lett.* **99**(25), 252904 (2011).
- <sup>18</sup>B. Xu, Y. Ye, Q.-M. Wang, and L. Eric Cross, *J. Appl. Phys.* **85**(7), 3753 (1999).
- <sup>19</sup>S. Gariglio, N. Stucki, J. M. Triscone, and G. Triscone, *Appl. Phys. Lett.* **90**(20), 202905 (2007).